NUCLEATION AND GROWTH OF HELIUM-VACANCY CLUSTERS IN IRRADIATED METALS. PART II. A GROUPING METHOD FOR AN APPROXIMATE SOLUTION OF TWO DIMENSIONAL KINETIC EQUATIONS DESCRIBING EVOLUTION OF POINT DEFECT CLUSTERS TAKING INTO ACCOUNT BROWNIAN MOTION OF THE CLUSTERS—S. I. Golubov, R. E. Stoller, S. J. Zinkle (Oak Ridge National Laboratory)*

OBJECTIVE

The objective of this work is to develop kinetic models describing the nucleation and evolution of radiation-induced defect clusters. Current work includes the modification of a previously-developed grouping method used to obtain a solution for the two dimensional kinetic equations describing gas assisted vacancy cluster formation in irradiated materials. The new model can account for the coalescence of clusters driven by Brownian motion.

SUMMARY

Nucleation, growth and coarsening of point defect clusters or secondary phase precipitates are of interest for many applications in solid-state physics. As an example, clusters nucleate and grow from point defects (PD) in solid under irradiation. In typical nucleation, growth and coarsening problems, a master equation (ME) is constructed that summarizes the large number of equations needed to describe the evolution process. When only the mobility of point defects and their reactions with the clusters are taken into account the ME takes the form of a differential equation known as the continuity equation in cluster size space. A new grouping method was developed by Golubov et al. for both the one-dimensional ME, which describes evolution of dislocation loops under irradiation or ageing, and the two-dimensional ME, which describes gas-assisted nucleation of voids or bubble formation in irradiated metals [1, 2]. However it has been shown that mobility of the clusters (e.g. He-vacancy) leading to coalescence, may play a key role in their evolution, particularly in the case of annealing of He implanted metals. The ME in the case becomes of the integro-differential type which complicates the numerical solution. The coalescence of clusters has been treated by different calculation methods (see e.g. [3-9]) but it has not been subjected to any specific grouping method of the type just described and this work intends to fill this gap. In the present work, the grouping method proposed by Golubov et al. [1] for the two-dimensional ME is generalized to take into account the coalescence of the clusters. An application of the method to the problem of helium bubble evolution which takes place during annealing of He implanted stainless steel is presented.

PROGRESS AND STATUS

Introduction

Precipitation of helium introduced into metals by (n,α) reactions that occur in fission and fusion reactors influence microstructure evolution materials. It has been established that helium atoms assist the nucleation and growth of cavities in irradiated materials leading to swelling and mechanical properties changes. The literature contains several partial treatments of the problem where both coarsening mechanisms, namely Ostwald ripening (see discussion in [1]) and bubble migration and coalescence [3-9] have been considered. However an accurate treatment of the second mechanism problem is complicated and most previous work has been done in a semi-quantitative way [7,13,14]. When calculating bubble coalescence under annealing conditions, it has commonly been assumed that bubbles maintain mechanical equilibrium during their evolution, which may not be the case. Moreover, very little has been done to calculate bubble evolution while taking into account both coarsening mechanisms simultaneously. It has been shown [1] that for the case when cluster evolution is driven by only mobility of point defects, the simplest and accurate grouping method may be obtained when size distribution function (SDF) within

---

*The work has been done in collaboration with A. M. Ovcharenko and C. H. Woo (Department of Mechanical Engineering, The Hong Kong Polytechnic University, Hong Kong).

a group is approximated by a linear function. Such an approximation maintains the identity of the grouped ME with the original one, while satisfying the conservation laws for both the total number of clusters and the total number of point defects accumulated in the clusters. However the calculation of bubble coalescence has not been subjected to any specific grouping method of the type mentioned. It appears that the grouping method developed in [1] can be generalized to take into account bubble migration and coalescence and this is the objective of the present work. It has been shown that in the framework of a generalized grouping method describing the evolution of the cluster SDF equal accuracy can be obtained for the general case when the evolution is driven simultaneously by cluster interactions with mobile point defects, and by Brownian motion of the clusters.

Master Equation

To describe the evolution of He-vacancy clusters driven by reactions with mobile point defects and Brownian motion of the clusters, the following ME has to be solved in the two-dimensional phase space of x, m

$$\frac{df(x,m,t)}{dt} + \nabla_x J_x(x,m,t) + \nabla_m J_m(x,m,t) = \frac{df(x,m,t)}{dt}_{|BM}, \tag{1}$$

where $f(x,m,t)$ and $J_x(x,m,t), J_m(x,m,t)$ are the SDF (the number density of clusters containing *x* vacancies and *m* He atoms) and fluxes of clusters in *x* and *m*-spaces, respectively. The fluxes are determined by the reactions of clusters with point defects

$$\begin{aligned} J_x(x,m,t) &= P_x(x,m,t) f(x,m,t) - Q_x(x+1,m,t) f(x+1,m,t), \\ J_m(x,m,t) &= P_m(x,m,t) f(x,m,t) - Q_m(x,m+1,t) f(x,m+1,t), \end{aligned} \tag{2}$$

where the coefficients $P_x(x,t)$, $Q_x(x,m,t)$, $P_m(x,t)$, and $Q_m(x,m,t)$ are the reaction rates for capture (*P*) and evaporation (Q) between the mobile point defects and clusters leading to a change in the cluster of size x and m, respectively.

The right hand side of the Eq. (1) represents the rate of change of the SDF caused by Brownian motion and coalescence. It may be expanded as follows:

$$\begin{aligned} \frac{df(x,m)}{dt}_{|BM} &= -f(x,m) \sum_{\substack{x'\geq 1, x'\neq x \\ m'\geq 0, m'\neq m}} \Lambda_{xm,x'm'} f(x',m') - 2f^2(x,m)\Lambda_{xm,xm} + \\ &\sum_{\substack{x'\leq x-2 \\ m'\leq m}} \sum_{\substack{x''\leq x-2 \\ m''\leq m}} \Lambda_{x'm',x''m''} f(x',m') f(x'',m'') \delta(x-x'-x'') \delta(m-m'-m'') = 0. \end{aligned} \tag{3}$$

In Eq. (3) $\Lambda_{x'm',x''m''}$ is the collision cross section between the clusters containing x', m' and x'', m'' vacancies and He atoms and $\delta(x)$ is the Kronneker delta. In the case of Brownian motion $\Lambda_{x'x'',m'm''}$ may be written in the following form:

$$\Lambda_{x'm',x''m''} = \left(48\pi^2/\Omega^2\right)^{1/3} \left[(x')^{1/3} + (x'')^{1/3}\right] \left[D_{x'm'} + D_{x''m''}\right], \tag{4}$$

where Ω is the atomic volume, $D_{x'm'}$ and $D_{x''m''}$ are diffusion coefficients of size x', m' and x'', m'' clusters. The first term on the right hand side of Eq. (3) describes the rate of decrease in number density of size x, m clusters via collision of the clusters with all other clusters except the x, m clusters. The second term describes coalescence of two x, m clusters. Note that a multiplier of 2 takes into account that the coalescence of the clusters leads to the disappearance of two clusters of the same size. The third term describes the formation of x, m clusters via collisions between smaller clusters which satisfy the equations:

$$x = x' + x'',\ m = m' + m''. \tag{5}$$

The ME in the form of Eq. (1) leads a set of rate equations for clusters of each size in the range of practical interest. It has already been pointed out [1,2] that for practical purposes it is necessary to consider clusters containing such a large number of point defects (or atoms) that the numerical solution of Eq. (1) becomes difficult. The grouping method developed in [1] permits the number of equations needing to be greatly thus providing a tool which can be useful for numerical solution of Eq.(1). Below the grouping method generalized to take into account coalescence of clusters is presented.

The Grouping Method

Following [1], the cluster SDF is divided into a series of groups with widths $\Delta x_i = x_i - x_{i-1}$, $\Delta m_j = m_j - m_{j-1}$, which include the clusters of the sizes

$$\begin{aligned} &x = x_{i-1} + k,\ \left(k = 1,..,\Delta x_i\right), \\ &m = m_{j-1} + n,\ \left(n = 1,..,\Delta m_j\right), \end{aligned} \tag{6}$$

respectively. The subscript i indicates the number of a group in $x-$space and the subscript j indicates the number of a group in $m-$space. Thus each group consists of $n_{i,j} = \Delta x_i \Delta m_j$ numbers of clusters of different sizes and is defined by the double index "*ij*".

Follow [1] let us approximate $f(x,m,t)$ by a linear function within a group i, j of the type

$$f_{i,j}(x,m) = L_0^{i,j} + L_{1x}^{i,j}(x - < x >_i) + L_{1m}^{i,j}(m - < m >_j). \tag{7}$$

where <> denotes the average number of vacancies and He atoms in the group of clusters. As can be seen from Eq. (7) each group of clusters is defined by three coefficients, $L_0^{i,j}, L_{1x}^{i,j}, L_{1m}^{i,j}$. Thus, the kinetic equation for the grouping method is formulated as a set of three equations for the coefficients in each cluster group. It has been shown [1] that in the case where evolution of the clusters is driven by only reactions between clusters and point defects, the equations for $L_0^{i,j}, L_{1x}^{i,j}, L_{1m}^{i,j}$ are given by

$$\frac{dL_0^{i,j}}{dt} = \frac{1}{\Delta x_i}\left[J_x(x_{i-1}, < m >_j) - J_x(x_i, < m >_j)\right] + \frac{1}{\Delta m_j}\left[J_m(< x >_i, m_{j-1}) - J_m(< x >_i, m_j)\right]. \tag{8}$$

$$\frac{dL_{1x}^{i,j}}{dt} = -\left(\frac{\Delta x_i - 1}{2\sigma_i^2 \Delta x_i}\right)\left\{ J_x(x_{i-1}, <m>_j) + J_x(x_i, <m>_j) - 2J_x(<x_i> - \frac{1}{2}, <m>_j) \right\}$$
$$+\frac{1}{\Delta m_j}\left\{ \left[J_m(<x>_i + 1, m_{j-1}) - J_m(<x>_i, m_{j-1})\right] - \left[J_m(<x>_i + 1, m_j) - J_m(<x>_i, m_j)\right] \right\}. \quad (9)$$

$$\frac{dL_{1m}^{i,j}}{dt}\Big|_{PD} = -\left(\frac{\Delta m_j - 1}{2\sigma_j^2 \Delta m_j}\right)\left\{ J_m(<x>_i, m_{j-1}) + J_m(<x>_i, m_j) - 2J_m(<x>_i, <m>_j - \frac{1}{2}) \right\}$$
$$+\frac{1}{\Delta x_i}\left\{ \left[J_x(x_{i-1}, <m>_j + 1) - J_x(x_{i-1}, <m>_j)\right] - \left[J_x(x_i, <m>_j + 1) - J_x(x_i, <m>_j)\right] \right\}. \quad (10)$$

where σ_i^2, σ_j^2 are the dispersions of cluster sizes in the group, which are given by

$$\sigma_i^2 = \frac{1}{\Delta x_i}\left[\sum_{\alpha=x_{i-1}+1}^{x_i} \alpha^2 - \frac{1}{\Delta x_i}\left(\sum_{\alpha=x_{i-1}+1}^{x_i} \alpha\right)^2\right],$$
$$\sigma_j^2 = \frac{1}{\Delta m_j}\left[\sum_{\alpha=m_{j-1}+1}^{m_j} \alpha^2 - \frac{1}{\Delta m_j}\left(\sum_{\alpha=m_{j-1}+1}^{m_j} \alpha\right)^2\right]. \quad (11)$$

For the case when Brownian motion of clusters takes place, the SDF is changed in accordance with the right hand side of Eq. (1). Thus, the final form of the kinetic equations in the framework of the grouping method has the form

$$\frac{dL_0^{i,j}}{dt} = \frac{dL_0^{i,j}}{dt}\Big|_{PD} + \frac{dL_0^{i,j}}{dt}\Big|_{BM},$$
$$\frac{dL_{1x}^{i,j}}{dt} = \frac{dL_{1x}^{i,j}}{dt}\Big|_{PD} + \frac{dL_{1x}^{i,j}}{dt}\Big|_{BM}, \quad (12)$$
$$\frac{dL_{1m}^{i,j}}{dt} = \frac{dL_{1m}^{i,j}}{dt}\Big|_{PD} + \frac{dL_{1m}^{i,j}}{dt}\Big|_{BM}.$$

To derive the rates $\frac{dL_0^{i,j}}{dt}_{|BM}, \frac{L_{1x}^{i,j}}{dt}_{|BM}, \frac{L_{1m}^{i,j}}{dt}_{|BM}$, the two following assumptions are made:

(a) diffusion coefficients of all clusters within a group are equal to each other

(b) collision of any cluster within a group *pq* with any cluster within a group $p'q'$ creates a cluster, which belongs to a single group *ij* satisfying the following inequalities

$$x_i - 1 < \left(<x>_p + <x>_{p'}\right) \le x_i,$$
$$m_j - 1 < \left(<m>_q + <m>_{q'}\right) \le m_j. \quad (13)$$

The first assumption leads to a simple situation in which the collision rates of any particular size cluster within a group with any size cluster within another group are equal to each other. As a result, clusters of all different size inside a group coalesce with the same rate, i.e. they can be considered as a bunch of single size clusters. Since the cross section for cluster coalescence is proportional to the product of the cluster densities, which are determined by the zero order coefficients $L_0^{i,j}$ only ($N_{i,j} = L_0^{i,j}\Delta x_i \Delta m_j$), the rate equation for the coefficient can be written similarly to that of Eq. (3):

$$\left(\frac{dL_0^{i,j}(t)}{dt}\right)_{\text{int}} = -\left(L_0^{i,j}(t)\right)^2 \Lambda_{ij,ij}\Delta x_i \Delta m_j - L_0^{i,j}(t)\sum_{k,n}\Lambda_{ij,kn}L_0^{k,n}(t)\Delta x_k \Delta m_n + \frac{1}{\left(\Delta x_i \Delta m_j\right)}\sum_{p,q}\sum_{p'q'}\Lambda_{pq,p'q'}L_0^{p,q}(t)L_0^{p',q'}(t)\Delta x_p \Delta m_q \Delta x_{p'}\Delta m_{q'}. \tag{14}$$

The only difference being that instead of the Kronneker delta in the last term on the right hand side, the indexes *pq* and $p'q'$ have to satisfy Eq. (13). The first term on the right hand side of Eq. (14) describes the rate of decrease of number density of the *ij* group clusters via collision of the clusters with all other clusters except clusters of same group. The second term describes coalescence of the *ij* group clusters with clusters in same group. Note that a multiplier of 2 accounts for coalescence of the clusters that leads to the disappearance of two clusters of the same group. The third term describes the formation of x, m clusters in *ij* group via collisions of clusters from smaller size groups.

In order to derive equations for the two other coefficients, $L_{1x}^{i,j}(t), L_{1m}^{i,j}(t)$, one needs to calculate the rate of change of the total number of *x* and *m* type defects accumulated in the group fed by the coalescence. These are given by [1]

$$S_{i,j} = \left(L_0^{i,j} < x >_i + L_{1x}^{i,j}\sigma_i^2\right)\Delta x_i \Delta m_j,$$
$$M_{i,j} = \left(L_0^{i,j} < m >_j + L_{1m}^{i,j}\sigma_j^2\right)\Delta x_i \Delta m_j, \tag{15}$$

Taking into account the assumption (a) mentioned above, it is clear that coalescence of the *ij* group clusters described by the first and second terms on the right hand side of Eq. (14) does not change the coefficients $L_{1x}^{i,j}(t), L_{1m}^{i,j}(t)$ since the change of values $S_{i,j}, M_{i,j}$ is fully described by the change of the coefficient $L_0^{i,j}$. However this is not the case for coalescence described by the third term on the right hand side of Eq. (14) since a sum of the average sizes of pq and $p'q'$ groups is not equal to the average size of resulting *ij* group. Taking into account conservation of the total number of *x* and *m* type of defects accumulated in pq , $p'q'$ and *ij* cluster groups, one can find the following equations for these coefficients:

$$\left(\frac{dL_{1x}^{i,j}(t)}{dt}\right)_{BM} = \frac{1}{\left(\Delta x_i \Delta m_j\right)\sigma_i^2}\sum_{p,q}\sum_{p',q'}\left\{\Delta x_p \Delta m_q \Delta x_{p'} \Delta m_{q'}\right.$$
$$\left.\Lambda_{pq,p'q'} L_0^{p,q}(t) L_0^{p',q'}(t)\left(< x >_p + < x >_{p'} - < x >_i\right)\right\},$$

(16)

$$\left(\frac{dL_{1m}^{i,j}(t)}{dt}\right)_{BM} = \frac{1}{\left(\Delta x_i \Delta m_j\right)\sigma_j^2}\sum_{p,q}\sum_{p',q'}\left\{\Delta x_p \Delta m_q \Delta x_{p'} \Delta m_{q'}\right.$$
$$\left.\Lambda_{pq,p'q'} L_0^{p,q}(t) L_0^{p',q'}(t)\left(< m >_q + < m >_{q'} - < m >_j\right)\right\}.$$

Note that similar to Eq. (14), the indexes *pq* and $p'q'$ in Eqs. (16) have to satisfy Eq. (13). Thus, the set of equations (14) and (16) complete the description of evolution of the cluster SDF caused by coalescence within the group method. Equations (12), (14) and (16) together with Eqs. (8)- (10) describe the evolution of SDF within the group approximation taking into account both point defects and cluster mobility. To illustrate the applicability of the method, these equations have been used to calculate the evolution of He bubbles taking place during ageing in pre-implanted stainless steel [10]. Note that the grouping method presented above can be used for both irradiation and ageing, so the calculations presented here consist two parts: (1) implantation of He atoms in the material and (2) annealing of the He-implanted material.

Evolution of He Bubbles Under Irradiation and Annealing

Model description

In order to use the grouping method to describe the evolution of He-vacancy clusters one needs to specify the fluxes $J_x(x,m,t), J_m(x,m,t)$, the diffusion coefficient for the Brownian motion of the clusters, and to set up the equations for mobile point defects with initial and boundary conditions. In Ref. [1] it was shown that for the case where concentrations of 3-D diffusing PDs, $C_v(t), C_i(t)$, are measured in atomic fractions, the rates $P_x\left(x,t\right)$ and $Q_x\left(x,m,t\right)$ in Eq. (2) may be written as follows

$$P_x(x) = wx^{1/3} D_v C_v(t),$$
$$Q_x(x,m) = wx^{1/3}\left[D_i C_i + D_v \exp\left(-E_v^b(x,m)/kT\right)\right] = Q_x^i(x,m) + Q_x^v(x,m), \tag{17}$$

where $w = \left(48\pi^2/\Omega^2\right)^{1/3}$, D_v, D_i are the diffusion coefficients of 3-D diffusing vacancies and interstitials, $E_v^b(x,m)$ is the binding energy of vacancy with a cluster of size *x* containing m gas atoms, k_B is the Boltzmann constant, and T is absolute temperature. The binding energy in Eq. (17) is given by

$$E_v^b(x,m) = E_v^f - \frac{\alpha}{x^{1/3}} + \left(\frac{m}{x}\right) Z\left(\frac{m}{x}, T\right) k_B T, \tag{18}$$

where E_v^f is the vacancy formation energy, $\alpha = 2\gamma\left(4\pi\Omega^2/3\right)^{1/3}$ and γ is the surface energy. The compressibility factor, $Z(T, m/x)$, is computed using the expression derived by Manzke and Trinkaus [11,12]

$$Z(T, m/x) = (1-\rho)\left(1+\rho-52\rho^2\right) + \frac{b}{V_m}\rho(1-\rho)^2 + Z_m\rho^2(3-2\rho), \tag{19}$$

where

$$\begin{aligned}
&\rho = \left(\frac{V_m}{\Omega}\right)\frac{m}{x},\\
&V_m = 56\mathrm{T}^{-1/4}\exp(-0.145\ \mathrm{T}^{1/4}),\\
&Z_m = 0.1225\ V_m\mathrm{T}^{\ 0.555},\\
&b = 170\mathrm{T}^{-1/3}\ -\ 1750\mathrm{T}^{-1}.
\end{aligned} \tag{20}$$

In Eq. (20) V_m is the He atomic volume is measured in cubic angstroms. Note that Eqs. (20) is written assuming that the volume of the cluster containing *x* vacancies, *V*, is equal to $V = x\Omega$.

In the second Eq. (2) $P_m(x,m,t)$ is the rate of helium absorption by an x,m cluster and $Q_m(x,m,t)$ is the rate of helium resolution from the clusters. The coefficients $P_m(x,m,t)$ and $Q_m(x,m,t)$ are used here in the simple form similar to that for vacancies in Eq. (17). Thus, in the present calculations $P_m(x,m,t)$ and $Q_m(x,m,t)$ are computed as:

$$\begin{aligned}
&P_m(x) = wx^{1/3}D_{He}C_{He},\\
&P_m(x) = wx^{1/3}D_{He}\exp\left(E_{res}/k_BT\right),
\end{aligned} \tag{21}$$

where $C_{He}(t)$ and D_{He} are the concentration and diffusion coefficient of He atoms by the interstitial mechanism, E_{res} is an activation energy for helium resolution from the clusters. Taking into account Eqs. (17) and (21), the evolution of mobile defect concentrations $C_v(t), C_i(t), C_{He}(t)$ may be presented as follows

$$\begin{aligned}
\frac{dC_v}{dt} = &\Big\{G_v + Q_m(1)f(1,1,t) + Q_x(2,0)f(2,0,t) +\\
&\sum_{x=2}^{\infty}\sum_{m=0}^{\infty}Q_x^v(x+1,m)f(x+1,m,t) + D_vC_{v0}Z_v\rho_d\Big\}\\
&-\left[\mu_RD_iC_iC_v + \mu_R^{He}D_{He}C_{He}C_v + D_vC_vZ_v\rho_d + P_x(1)f(1,0,t) + \sum_{x=1}^{\infty}\sum_{m=0}^{\infty}P_x(x)f(x,m,t)\right],
\end{aligned} \tag{22}$$

$$\frac{dC_i}{dt} = G_i - \mu_R D_i C_i C_v - D_i C_i Z_i \rho_d - \sum_{x=2}^{\infty} \sum_{m=0}^{m_{\max}} Q_x^i(x) f(x,m,t) - Q_x^i(1) \sum_{m=1}^{m=m_0} f(1,m). \tag{23}$$

$$\begin{aligned} \frac{dC_{He}}{dt} &= \left\{ G_{He} + \sum_{x=2}^{\infty} \sum_{m=1}^{m_{\max}} Q_m(m) f(x,m,t) + \sum_{m=1}^{m=m_0} \left[Q_m(m) + m Q_x^i(1) \right] f(1,m) \right\} \\ &- \left[\mu_R D_{He} C_v C_{He} + D_{He} C_{He} Z_{He} \rho_d + \sum_{x=2}^{\infty} \sum_{m=0}^{m_{\max}-1} P_m(x) f(x,m,t) + P_m(1) \sum_{m=1}^{m=m_0-1} f(1,m) \right], \end{aligned} \tag{24}$$

where G_v, G_i, G_{He} are the generation rates of vacancies, self interstitial atoms (SIAs) and He atoms, respectively, μ_R is the coefficient describing the recombination reaction between SIA and vacancy, Z_v, Z_i are the capture efficiencies of dislocations for vacancies and SIAs, respectively, ρ is the dislocation density, C_{v0} is the thermal equilibrium vacancy concentration, m_0 is the maximum number of He atoms associated with a single vacancy (see e.g. [15-17]). The generation rates vacancies and SIAs are given by

$$\begin{aligned} G_v &= G_{NRT}(1-\varepsilon_r), \\ G_i &= G_{NRT}(1-\varepsilon_r), \end{aligned} \tag{25}$$

where G_{NRT} is the generation rate calculated using the NRT model, and ε_r is a fraction of the point defects recombined during cooling phase of cascades.

The migration of the clusters is assumed to be caused by mass transport on the bubble surface (see e.g. Ref. [18])

$$D_{ij} = \frac{3}{2\pi} D_S \left(\frac{\Omega^{1/3}}{< r >_i} \right)^4, \tag{26}$$

where $D_S = D^{(0)} \exp(-E_S / k_B T)$ is the surface diffusion coefficient, $< r >_i$ is the mean radius of the *ij* group of cluster, and $< r >_i = \left(\frac{3\Omega}{4\pi} < x >_i \right)^{1/3}$.

Eqs. (8)-(10), (12), (14) and (16)- (26) have been used to calculate He bubble evolution in a stainless steel under irradiation and annealing.

Experimental data and parameters used in the calculations

As discussed in Ref. [10], specimens of model austenitic alloy P7 (Fe-17Cr-16.7Ni-2.5Mo) were implanted with a 10 to 50 appm He at room temperature and subsequently annealed for one hour at temperatures between 600 and 900°C. The temperature during implantation was <200°C and the He implantation level in specimens used for the annealing varied between 32 and 47 appm. Helium bubble data obtained after one-hour annealing are summarized in Table 1.

Table 1. Summary of bubble microstructures observed after 40 appm helium implantation in solution-annealed P7 and subsequent annealing for one hour [10]

Helium implanted (appm)	T (^{o}C)	Bubble density ($10^{21}m^{-3}$)	Average bubble radius (nm)	Swelling
32	600	-	-	
44	700	8.25	0.82	$1.82*10^{-5}$
37	750	6.33	1.09	$3.2*10^{-5}$
47	800	6.66	1.57	$9.7*10^{-5}$
41	900	2.15	1.99	$6.7*10^{-5}$

As can be seen from the table, bubbles remained invisible after annealing at 600°C. At higher temperatures bubble evolution follows normal coarsening, i.e. the average size of bubbles increases and density decreases with increasing annealing temperature. Note that the small increase in bubble density between 750 and 800°C probably is a result of the higher level of implanted helium in the specimen used for annealing (see calculated helium content at this temperature in Table 1 in [10]).

It is interesting to note that swelling (see last column in Table 1) at all temperatures is very close to that introduced during helium implantation (about $4.0*10^{-5}$ assuming that all implanted He atoms survived in a He-vacancy cluster). Thus one may conclude that He emission from bubbles at all temperatures is low

The calculations in the present work have been done to illustrate the capability of the grouping method. Thus to simplify calculations the implantation temperature is chosen to be 100°C and the helium implantation level is considered to be equal to 40 appm in all specimens. Accordingly, the He implantation parameters used in our calculations are summarized in Table 2.

Table 2. The He implantation parameters in solution-annealed P7 used in the calculations

Helium generation rate, G_{He}	$2.0*10^{-3}$ appm/s
Implantation temperature	100°C
Displacement rate during implantation, G_{NRT}	$5.0*10^{-7}$ dpa/s
Implantation time	$2.0*10^{4}$s
Displacement dose	$1.0*10^{-2}$ dpa
Helium implantation level	40 appm

The calculations have been performed in two steps:

1. Helium pre-implantation regime, which is described by the concurrent processes of Frenkel pair production and He implantation
2. Calculations of bubble evolution during thermal annealing at a given temperature to predict the microstructure obtained.

The initial conditions for the mobile defects and boundary conditions for the SDF for step 1 have the following form:

$$
\begin{aligned}
&C_v(t)_{|t=0} = C_{v0}, \\
&C_i(t=0)_{|t=0} = C_{He}(t)_{|t=0} = 0, \\
&f(x,m,t)_{|t=0} = C_{v0}\delta(x-1)\delta(m), \quad (x \geq 1), \\
&f(x=1,0,t) = C_v(t), \quad f(x=\infty,m,t) = 0.
\end{aligned}
\tag{27}
$$

In addition, it is assumed that the smallest clusters (x=1) are immobile and can be filled with up to 4 helium atoms (see e.g. Ref. [15-17]). Material parameters used in the calculations are given in Table 3.

Table 3. Parameters used in the calculations

Recombination fraction, ε_r	0.75
Effective displacement rates, $G_{NRT}(1-\varepsilon_r)$	$1.25 * 10^{-7}$ dpa/s
Helium generation rate, G_{He}	$2.0*10^{-3}$ appm/s
Recombination coefficients, $\mu_R = \mu_R^{He}$	$5.0*10^{+20}$ m^{-2}
Atomic volume, Ω	$1.15*10^{-29}$ m^{-3}
Vacancy diffusion coefficient, D_v pre-exponential factor migration energy	 $8.0*10^{-05}$ m^2/s 1.40 eV
SIA diffusion coefficient, D_i pre-exponential factor migration energy	 $8.0*10^{-06}$ m^2/s 0.15 eV
He atom diffusion coefficient, D_{He} pre-exponential factor migration energy	 $8.0*10^{-06}$ m^2/s 0.15 eV
Dislocation density, ρ_d	10^{13} m^{-2}
He resolution energy, E_{res}	2.3 eV
Surface energy, γ	(3.4-1.4*T/1000) J/ m^2
Dislocation capture efficiency for vacancies, Z_v	1.00
Dislocation capture efficiency for SIAs, Z_i	1.25
Dislocation capture efficiency for He atoms, Z_{He}	0
Rate of radiation resolution, A	0
Surface diffusion coefficient, D_S pre-exponential factor, $D^{(0)}$ migration energy	 $(1.6*10^{-6}$-$8*10^{-5})$ m^2/s 1.40 eV

Results

Cluster evolution during implantation

As mentioned above, the first step in the calculations is to use the set of equations for the SDF formulated above within the grouping method to calculate helium implantation at 100°C with the irradiation parameters given in Table 1. Since the implantation temperature is below recovery stage three, vacancies at this temperature are immobile. The evolution of He-vacancy clusters therefore is driven by the mobility of interstitial He and self interstitial atoms. The calculations are carried to a dose of 10^{-2} dpa where the He concentration reached a level of 40 appm. It is found that all He atoms are accumulated in clusters of the smallest size *x= 1*. The SDF obtained during the calculations is used as input to the subsequent calculations of cluster evolution during annealing at temperatures of 600° C and above.

Cluster evolution during annealing at 600°C

As can be seen from Table 1, helium bubbles have not been found in specimens annealed at 600° C for one hour. Thus, the calculations of annealing at this temperature could be used to test the efficiency of different mechanisms and parameters used for causing cluster evolution. The calculated results for the number density and average size of the clusters obtained for different values of the cluster mobility are presented in Figs. 1 and 2. The upper curves in Fig.1 correspond to the total number density of the clusters, and the bottom ones correspond to the number density of visible clusters, i.e. clusters with radius larger than 0.5 nm.

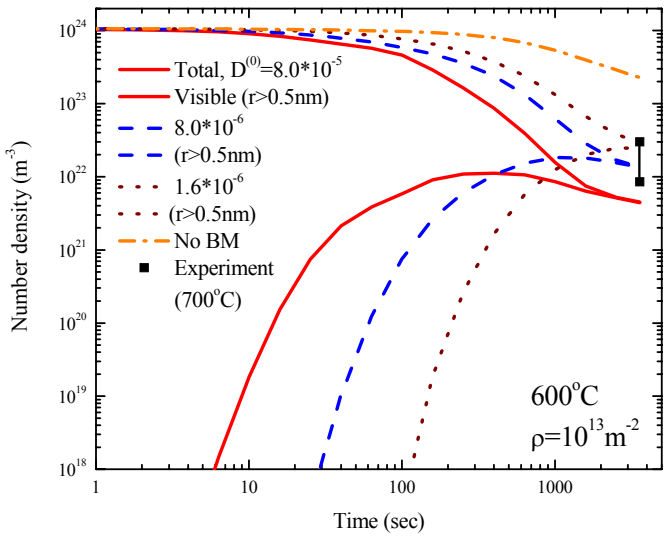

Fig. 1. Calculated time dependence of the bubble density obtained for annealing at 600°C at different magnitudes of bubble diffusivity.

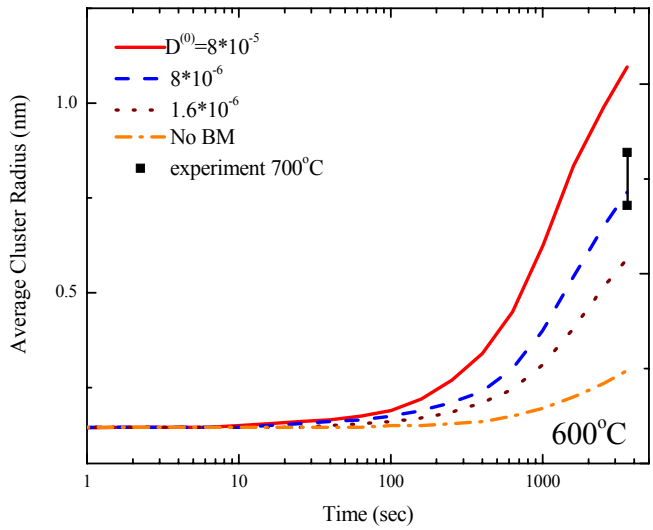

Fig. 2. Calculated time dependence of the average bubble radius obtained for annealing at 600°C with different values of bubble diffusivity.

It can be seen from the Figs. 1 and 2 that in the case where the cluster mobility is not taken into account (marked on the plot as “No BM”) there is very limited cluster evolution. This is related to the fact that without Brownian motion the driving force for cluster evolution is emission of He atoms from the clusters which is very inefficient at this temperature. Thus, one may conclude that cluster mobility under annealing is the main driving force for cluster evolution. As reference points on Fig. 1 and 2, the measured values of bubble density and size after annealing at 700°C are also presented. Comparing the calculated results with the reference points in Fig. 2, one may conclude the calculation results obtained for $D^{(0)} = 1.6*10^{-6} m^2 / s$ agrees with the observations since in this case the bubble size is too small to be detected by TEM.

The calculated size distribution functions of bubbles after annealing for one hour at 600°C for different values of cluster mobility are presented in Figs. 3a, 3b and 3c.

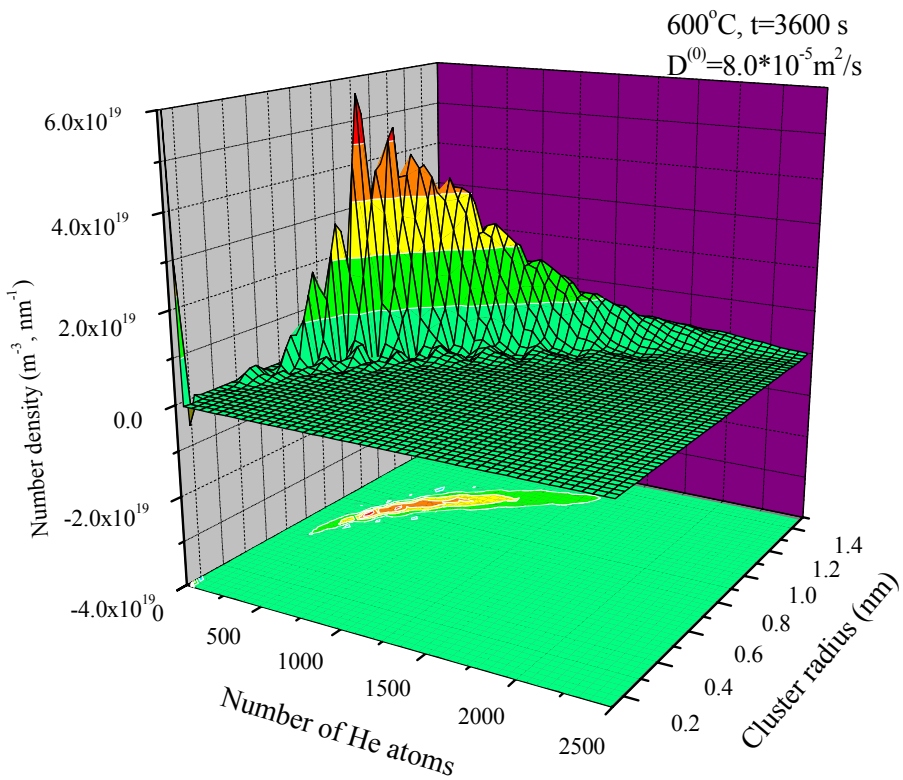

Fig. 3a. Size distribution function of gas bubbles for simulated annealing for one hour at 600°C with the pre-exponential factor equal to $8.0*10^{-5}$ m^2/s.

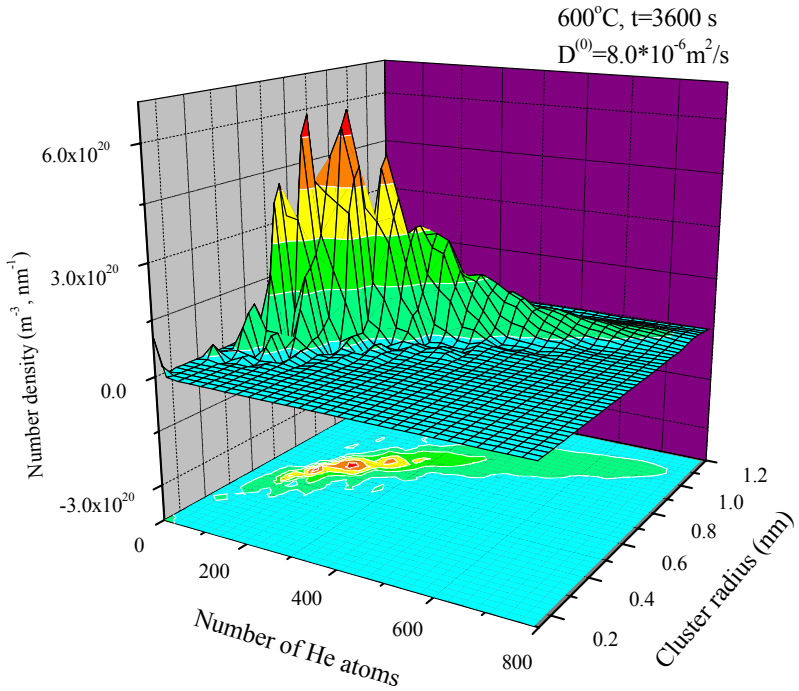

Fig. 3b. Size distribution function of gas bubbles for simulated annealing for one hour at 600°C with the pre-exponential factor equal to $8.0*10^{-6}$ m^2/s.

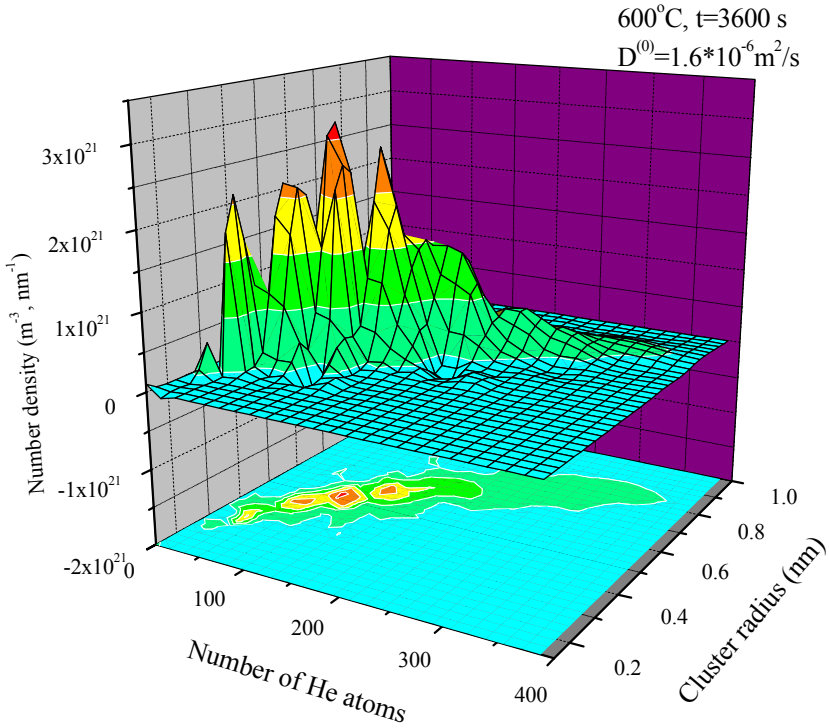

Fig. 3c. Size distribution function of gas bubbles for simulated annealing for one hour at 600°C with the pre-exponential factor equal to $1.6*10^{-5}$ m^2/s.

As can be seen from Fig. 3, the shape of the SDF in all cases is quite similar; all clusters are concentrated along a certain trajectory in *x,m*-space. Close analysis shows that along this trajectory, the gas pressure in the clusters is nearly constant, i.e. all clusters are over- pressurized with respect to the equilibrium value caused by surface tension ($2\gamma / r_{cl}$). Such a situation may be rationalized by taking into account that when coalescence of clusters is the main mechanism of cluster evolution, the total number of vacancies and He atoms accumulated in clusters are conserved keeping the ratio $< m > / < x >$ inside clusters close to a constant. This in turn leads to constant pressure inside the clusters. As a result, the mean cluster size does not follow the law $< r > \sim t^{1/5}$, which is predicted for the case when all bubbles are considered to be in equilibrium. The actual increase in bubble size is found to be slower (about $< r > \sim t^{1/8}$) because there is a lack of vacancies to produce a more rapid size increase. This shows that models for bubble evolution under annealing condition suggested in the past (see e.g. Ref. [3-6]), which considered the process as an evolution of equilibrium bubbles only, are not valid in the case under consideration. Note that a similar situation is likely to be valid at all annealing temperatures up to 900°C since, as pointed out above, the total volume of bubbles after annealing in all cases is close to that introduced in the crystal during helium implantation.

Note that the one-dimensional SDF, $f(x)$, which is normally measured with TEM, can be easily calculated by using the two-dimensional SDF by summation over the parameter *m*, $f(x) = \sum_m f(x,m)$. An example of the one-dimensional SDF, which corresponds to the two-dimensional SDFs presented in Fig. 3, is presented in Fig. 4.

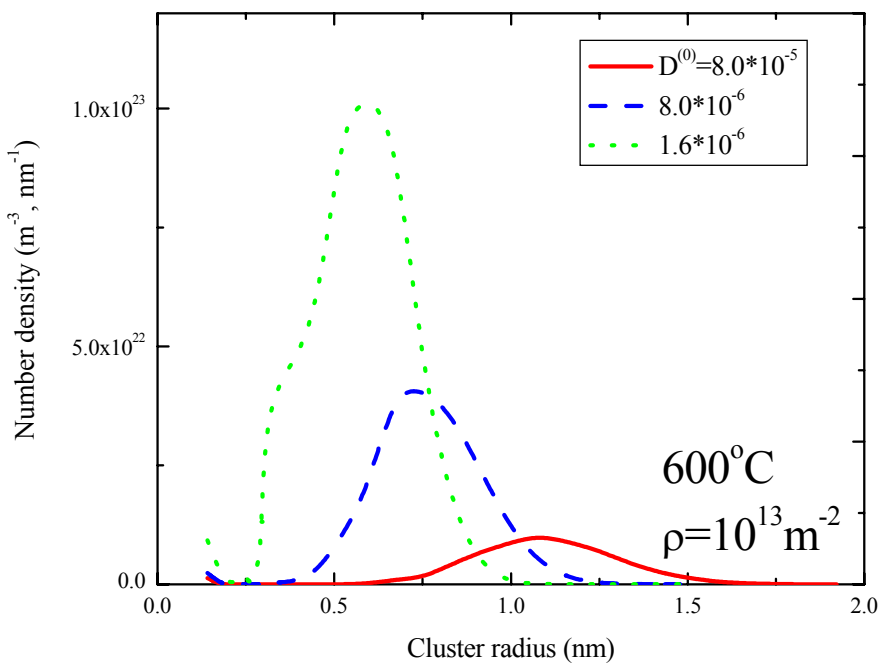

Fig. 4. One-dimensional size distribution function of gas bubbles, which corresponds to that presented on Fig. 3 calculated by summation over the parameter *m*, $f(x) = \sum_m f(x,m)$.

Cluster evolution during annealing at 700°C

Calculations of the He-vacancy cluster evolution during annealing at 700°C have also been performed for different values of the cluster diffusivity. The time evolution of SDF for $D^{(0)}$=8.0*10^{-6} m^2/s is presented in Figs. 5 for annealing times of 400 (a), 1600 (b) and 3600 (c) seconds. As can be seen from the plots, the evolution of bubbles exhibits the same trend as was found for an annealing temperature 600°C. The SDFs located in *x,m* – space follow a certain trajectory, which is the region where all clusters are over-pressurized.

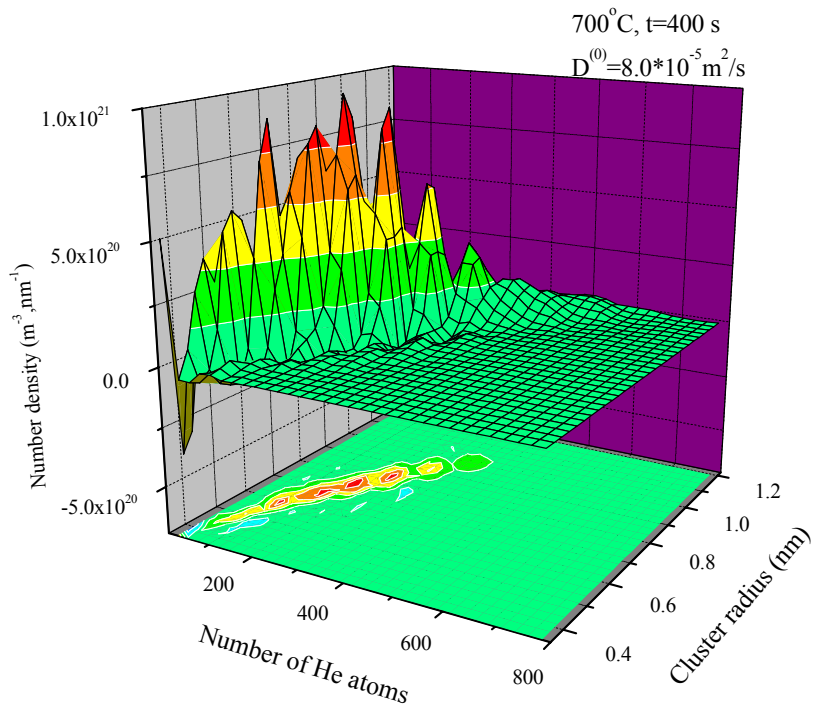

Fig. 5a. Size distribution function of gas bubbles at 700°C calculated under annealing for 400 sec with the pre-exponential factor equal to 8.0*10^{-6} m^2/s.

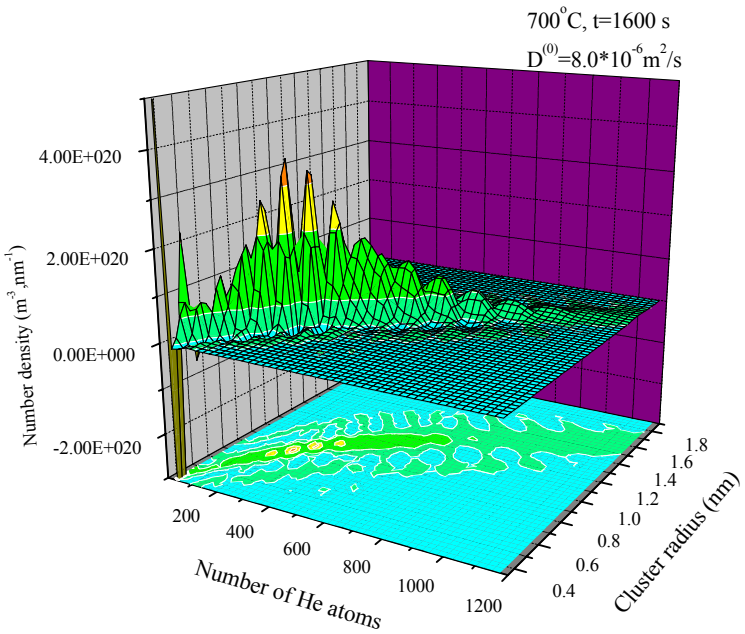

Fig. 5b. Size distribution function of gas bubbles at 700°C calculated under annealing for 1600 sec with the pre-exponential factor equal to $8.0*10^{-6}$ m^2/s.

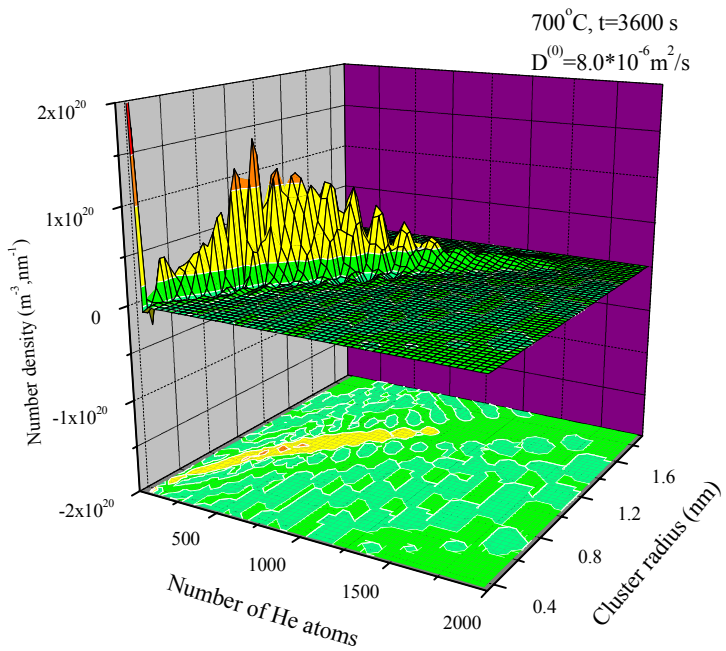

Fig. 5c. Size distribution function of gas bubbles at 700°C calculated under annealing for 3600 sec with the pre-exponential factor equal to $8.0*10^{-6}$ m^2/s.

The calculated results for number density and average size of clusters obtained with the different cluster nobilities are presented in Fig. 6 and 7. Similar to Fig. 1, the upper curves in Fig. 6 correspond to the total number of clusters, whereas the lower curves correspond to the density of visible clusters (r>0.5 nm). As can be seen from the plots the calculated results obtained with the smallest value of cluster diffusivity, ($D^{(0)}=1.6*10^{-6}m^2/s$), fit the experimental data for both the density of the clusters and their size. Thus, one can conclude that the calculated results obtained for $D^{(0)}=1.6*10^{-6}m^2/s$ agree reasonably well with the experimental observations in the temperature range of 600-700^{0}C. The calculations of bubble evolution during annealing at temperatures 800 and 900^{0}C are still in progress.

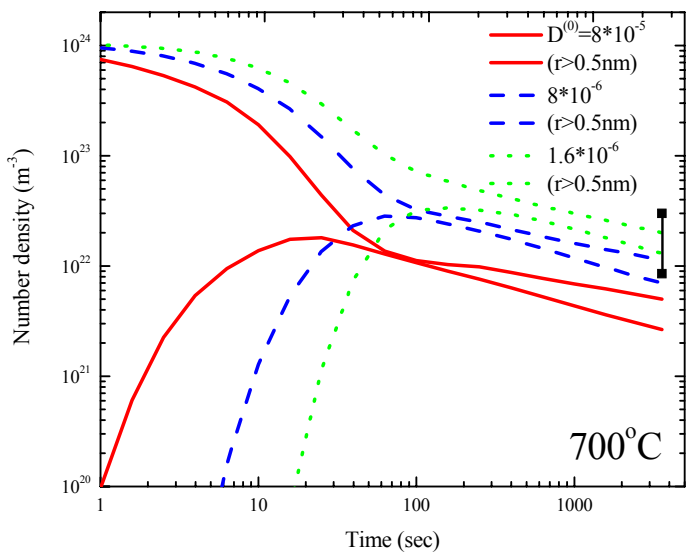

Fig. 6. Time dependence of the bubble density during annealing at 700°C as calculated with different values of the bubble diffusivity.

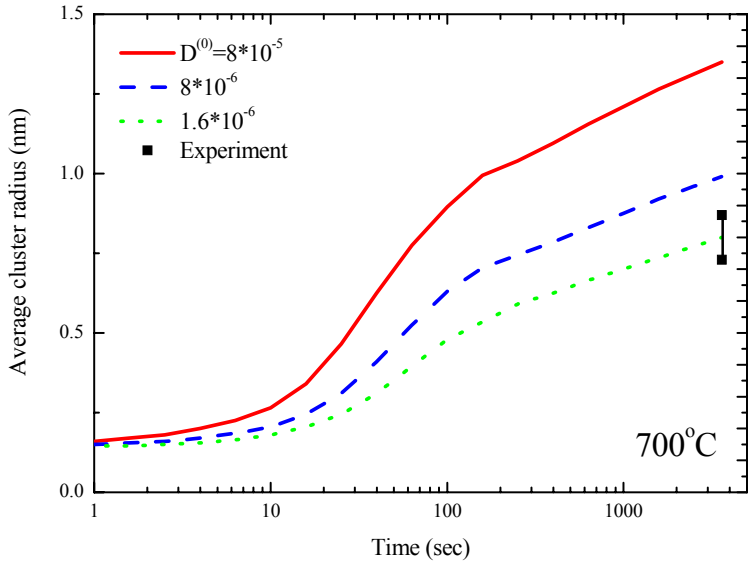

Fig. 7. Time dependence of the mean bubble radius during annealing at 700°C as calculated with different values of the bubble diffusivity.

Conclusions

A grouping method for an approximate solution of two dimensional kinetic equations describing the evolution of point defect clusters has been developed that takes into account Brownian motion of the clusters. It can be used to describe gas-assisted nucleation of voids, bubbles or secondary phase precipitates. It may be shown that the method can be easily generalized for ME of higher dimensionality.

The method was used to describe bubble evolution taking place during annealing in helium implanted (40 appm) austenitic steel, were it was found that that Brownian motion of the clusters is the main mechanism driving He-vacancy cluster evolution during annealing in the case under consideration. Surface diffusion provides a mechanism for cluster mobility, which leads to reasonable agreement between the calculated results and experimental observations for bubble evolution, at least in a temperature range of 600-700^{0}C.

References

[1] S. I. Golubov, R. E. Stoller, and S. J. Zinkle, Fusion Materials Semiannual Progress Report for Period Ending December 31, 2002, DOE/ER-0313/33, U.S. Department of Energy, 155.

[2] S.I. Golubov, A. M. Ovcharenko, A. V. Barashev, and B. N. Singh, Philos. Mag. Series A. 81, No. 3 (2001) 643-658.

[3] E. E. Gruber, In: Radiation-Induced Voids in Metals, Eds. J. W. Corbet and L. C. Iannielo, USAEC-CONF.71061, Albany (1972) 663.

[4] G. W. Greenwood and M. V. Speight, J. Nucl. Mater. 10 (1963) 140.

[5] M. V. Speight, J. Nucl. Mater. 12 (1964) 216.

[6] E. E. Gruber, J. Appl. Phys. 15 (1967) 243.

[7] P. J. Goodhew and S. K. Tyler, Proc. of the R. Soc. of Lond. A377 (1981) 151.

[8] A. J. E. Foreman and B. N. Singh, J. Nucl. Mater. 141-143 (1986) 672.

[9] V. F. Chkuaseli, J. Nucl. Mater. 188 (1992) 258.

[10] R. E. Stoller and G. R. Odette, Radiation Induced Changes in Microstructure: 13th International Symposium (Part I), ASTM STP 955, Eds. F. A. Garner, N. H. Packan, and A. S. Kumar, ASTM, Philadelphia (1987) 371.

[11] R. Manzke, W. Jäger, H. Trinkaus, G. Crecelius, and R. Zeller, Solid State Communications 44, No. 4 (1982) 481.

[12] H. Trinkaus, Rad. Effects 78 (1983) 189.

[13] B. N. Singh and H. Trinkaus, J. Nucl. Mater. 186 (1992) 153.

[14] H. Trinkaus and B. N. Singh, J. Nucl. Mater. 323 (2003) 229.

[15] Van Veen, Mater. Sci. Forum 15-18 (1987) 3.

[16] W. D. Wilson, C. L. Bisson, and M. I. Baskes, Phys. Rev. B 24 (1981) 5616.

[17] B. Adams and W. G. Wolfer, J. Nucl. Mater. 106 (1989) 235.

[18] D. R. Olander, Fundamental Aspects of Nuclear Reactor Fuel Elements, TID-26711-P1, (1976) 236.